Journal of Computational Physics 370 (2018) 25–42

Contents lists available at ScienceDirect

Journal of Computational Physics

www.elsevier.com/locate/jcp

Partitioned averaged vector field methods

Wenjun Cai [a], Haochen Li [b], Yushun Wang [a,*]

[a] Jiangsu Key Laboratory for NSLSCS, School of Mathematical Sciences, Nanjing Normal University, Nanjing, 210023, China
[b] School of Mathematical Sciences, Peking University, Beijing, 100871, China

ARTICLE INFO

Article history:
Received 7 December 2017
Received in revised form 23 April 2018
Accepted 5 May 2018
Available online 8 May 2018

Keywords:
Hamiltonian system
Energy-preserving scheme
Averaged vector field method
Discrete gradient method

ABSTRACT

The classic second-order averaged vector field (AVF) method can exactly preserve the energy for Hamiltonian systems. However, the AVF method inevitably leads to fully-implicit nonlinear algebraic equations for general nonlinear systems. To address this drawback and maintain the desired energy-preserving property, a first-order partitioned AVF method is proposed which first divides the variables into groups and then applies the AVF method step by step. In conjunction with its adjoint method we present the partitioned AVF composition method and plus method respectively to improve its accuracy to second order. Concrete schemes for two classic model equations are constructed with semi-implicit, linear-implicit properties that make considerable lower cost than the original AVF method. Furthermore, additional conservative property can be generated besides the conventional energy preservation for specific problems. Numerical verification of these schemes further conforms our results.

1. Introduction

We consider a Hamiltonian system of the form

$$\dot{z} = f(z) = S_m \nabla H(z), \tag{1.1}$$

where $z \in \mathbb{R}^m$, S_m is a $m \times m$ skew-symmetric constant matrix, and $H(z)$ is a Hamiltonian assumed to be sufficiently differentiable. The most relevant characters of the system (1.1) are the symplecticity and energy conservation along any continuous flows.

At a discrete level, attempts to incorporate the conservation of both quantities will clash with two nonexistence results in [1,2], which state that the only symplectic method (as B-series) that conserves the Hamiltonian for arbitrary $H(z)$ is the exact flow of the differential equation. Although there exist methods that inherit both feathers in a weak sense such as the symplectic-energy–momentum integrators by using time-adaptive steps and the energy–momentum conserving algorithms by introducing an extra free parameter [3], symplectic integrators and energy-preserving schemes constitute two individual lines to construct geometric numerical integration methods for Hamiltonian systems (see the monographs [4–6] and the more recent ones [7,8]).

Although the numerical solution of symplectic integrators exhibits long-time behavior, it was observed that symplecticity alone can only assure, at most, the conservation of quadratic Hamiltonian functions, unless they are coupled with some projection procedure. For general Hamiltonian, conservation cannot be assured. A way to get rid of this problem is to directly

* Corresponding author.
E-mail address: wangyushun@njnu.edu.cn (Y. Wang).

https://doi.org/10.1016/j.jcp.2018.05.009
0021-9991/

look for energy-preserving methods, able to provide an exact conservation of the Hamiltonian function along the numerical trajectory. The early energy-preserving methods include the projection methods [9] and the discrete gradient methods [10]. However, both these algorithms require the input of the concrete form of the Hamiltonian function. Recently, a new class of energy-preserving methods called averaged vector field (AVF) method was introduced in [11]. One of remarkable advantages of the AVF method is that it only requires evaluations of the vector field. The user does not even need to know that the specified vector field $f(z)$ is Hamiltonian, but if it is, its energy will be preserved. The AVF method is first written down in [10] as a specific discrete gradient method by taking a mean-value discrete gradient as the discrete counterpart of the gradient operator. Later on, the AVF method has been further related to other energy-preserving methods.

For instance, the AVF method is a limit case of second-order Hamiltonian boundary value methods (HBVMs), setting the number of stages of its Butcher tableau tending to infinity [12]. Furthermore, such a method is equivalent to the discrete partial derivative method (DPDM) providing the Hamiltonian does not contain cross-product terms of solution and its partial derivatives [13]. Additionally, the AVF method has been analyzed in the framework of B-series [11] and prompted intensive studies on energy-preserving B-series methods [14–17]. Moreover, for PDEs with constant dissipative structure, the AVF method can also preserve the correct monotonic decrease of energy [18].

For ordinary differential equations (1.1), the second-order AVF method is defined by

$$\begin{aligned}\frac{z^{n+1}-z^n}{\tau} &= \int_0^1 f(\xi z^{n+1}+(1-\xi)z^n)\mathrm{d}\xi \\ &= S_m \int_0^1 \nabla H(\xi z^{n+1}+(1-\xi)z^n)\mathrm{d}\xi,\end{aligned} \tag{1.2}$$

where τ denotes the time step. Using the fundamental theorem of calculus and the skew-symmetry of S_m, the Hamiltonian energy is precisely conserved at every time step, that is $H(z^{n+1}) = H(z^n)$. For polynomial Hamiltonians, the integral can be evaluated exactly, and the implementation is comparable to that of the implicit mid-point rule. When the Hamiltonian energy is a quadratic function, the resulting AVF scheme is linearly implicit and therefore can be efficiently solved. But this is not the case to reflect the merit of the AVF method since any symplectic Runge–Kutta method can also achieve the energy conservation for quadratic Hamiltonians [6]. Under most circumstances, the evaluation of the integration in (1.2) leads to a nonlinear function of z^{n+1} which further constitutes a fully implicit numerical scheme. The iterative processes are then inevitably required such that the computational complexity will be evidently increased, especially for the application on Hamiltonian PDEs.

The main aim of this paper is to construct a more efficient AVF based method. Instead of imposing the mean-value discrete gradient along the direct path $\gamma\colon z^n \to z^{n+1}$, we first divide this single path into several subpaths $\gamma_i\colon z_i^n \to z_i^{n+1}$, where the subscript represents the vector component of z. Then the mean-value discrete gradient method is applied on one subpath γ_i at a time. We denote this method as a partitioned AVF (PAVF) method which can also automatically preserve arbitrary Hamiltonian energy of system (1.1). Comparing with the AVF method (1.2), the resulting schemes of the partitioned AVF method are much simpler according to the concrete expressions which reduces the original fully implicit schemes to semi-implicit or linearly implicit schemes and therefore significantly improve the computational efficiency. Although such a method is only of first-order accuracy, in conjunction with its adjoint we further present the partitioned AVF composition (PAVF-C) method and the partitioned AVF plus (PAVF-P) method that both achieve second-order accuracy and energy-preserving property. Thanks to the great advantage of the PAVF method, even by its composition the PAVF-C method still has much lower cost than the direct AVF method. Although the computational efficiency of the PAVF-P method is comparable to the AVF method, it may possess additional conservative quantities that the AVF method cannot preserve.

This paper is organized as follows. In section 2, we present the partitioned AVF method and derive its energy-preserving property. The adjoint of this method as well as the induced partitioned AVF composition and plus methods are also proposed. Numerical schemes for Hamiltonian ODEs and PDEs are constructed and tested in section 3, including the Hénon–Heiles system and the Klein–Gordon–Schrödinger equation. We compare the original AVF method and our partitioned version methods in both the invariant preservation and computational cost. Concluding remarks are given in Section 4.

2. The partitioned AVF methods

For illustration, we consider the Hamiltonian system (1.1) when m is an even number, denoting $m = 2d$. Without generality the grouping strategy is simply choosing in sequential order, i.e., $z = (p,q)^T = (z_1, z_2, \ldots, z_d; z_{d+1}, z_{d+2}, \ldots, z_m)^T$. Accordingly, the original system (1.1) can be rewritten as

$$\begin{pmatrix}\dot{p}\\ \dot{q}\end{pmatrix} = S_{2d}\begin{pmatrix}H_p(p,q)\\ H_q(p,q)\end{pmatrix}, \quad p,q \in \mathbb{R}^d. \tag{2.1}$$

The present Hamiltonian $H(p,q)$ is still conserved along any continuous flow, that is

$$\frac{\mathrm{d}H(p(t),q(t))}{\mathrm{d}t} = H_p(p,q)^T\dot{p} + H_q(p,q)^T\dot{q} = \nabla H(p,q)^T S_{2d}\nabla H(p,q) = 0.$$

Then the so-called partitioned AVF (PAVF) method for the Hamiltonian system (2.1) is defined by

$$\frac{1}{\tau}\begin{pmatrix} p^{n+1}-p^n \\ q^{n+1}-q^n \end{pmatrix} = S_{2d}\begin{pmatrix} \int_0^1 H_p(\xi p^{n+1}+(1-\xi)p^n, q^n)\mathrm{d}\xi \\ \int_0^1 H_q(p^{n+1}, \xi q^{n+1}+(1-\xi)q^n)\mathrm{d}\xi \end{pmatrix}. \tag{2.2}$$

Theorem 2.1. *The PAVF method (2.2) preserves the Hamiltonian $H(p,q)$ of the system (2.1) exactly, and satisfies*

$$\frac{1}{\tau}(H(z^{n+1}) - H(z^n)) = 0.$$

Proof. Taking the scalar product with $(\int_0^1 H_p(\xi p^{n+1}+(1-\xi)p^n, q^n)^T\mathrm{d}\xi, \int_0^1 H_q(p^{n+1}, \xi q^{n+1}+(1-\xi)q^n)^T\mathrm{d}\xi)^T$ on both sides of (2.2), using the Fundamental Theorem of Calculus and the skew-symmetry of S_{2d}, we obtain

$$\begin{aligned}
0 &= \frac{1}{\tau}\int_0^1 H_p(\xi p^{n+1}+(1-\xi)p^n, q^n)^T\mathrm{d}\xi(p^{n+1}-p^n) \\
&\quad + \frac{1}{\tau}\int_0^1 H_q(p^{n+1}, \xi q^{n+1}+(1-\xi)q^n)^T\mathrm{d}\xi(q^{n+1}-q^n) \\
&= \frac{1}{\tau}\int_0^1 \frac{\mathrm{d}}{\mathrm{d}\xi}\big[H(\xi p^{n+1}+(1-\xi)p^n, q^n) + H(p^{n+1}, \xi q^{n+1}+(1-\xi)q^n)\big]\mathrm{d}\xi \\
&= \frac{1}{\tau}\big[H(p^{n+1},q^n) - H(p^n,q^n) + H(p^{n+1},q^{n+1}) - H(p^{n+1},q^n)\big] \\
&= \frac{1}{\tau}(H(p^{n+1},q^{n+1}) - H(p^n,q^n)) = 0. \quad \square
\end{aligned}$$

Remark 2.1. The PAVF methods (2.2) are one-step methods of order one.

Remark 2.2. If the system (2.1) is a separable Hamiltonian system of the form $H(p,q) = H_1(p) + H_2(q)$, then the PAVF method (2.2) is equivalent to the AVF method (1.2). However, the Hamiltonian system (2.1) is not separable in general which can just reflect the major advantage of the PAVF method. The key strategy of the PAVF method is to separate variables in cross-product terms into different groups and apply the AVF method only for one group during each step, which lead to much simper schemes that usually require less computational effort than the conventional AVF method. Particularly, the corresponding schemes can be linearly implicit at least for a part of the entire equation system which dramatically reduces the iteration scale or even avoid the nonlinear iteration completely. We will demonstrate this advantage through finite and infinite-dimensional Hamiltonian systems in the following part, respectively.

Remark 2.3. When the Hamiltonian H is a polynomial of degree m, the AVF method is equivalent to a Runge–Kutta method with the Butcher matrix $A = cb^T$, where $c = (c_1, \cdots, c_s)$ and $b = (b_1, \cdots, b_s)$ are nodes and weights of a quadrature rule which is exact for polynomials of degree $m-1$. Similarly, we can also replace the integrals in the PAVF method with numerical quadratures of sufficiently high order. However, the result method cannot be classified as the Runge–Kutta method or the partitioned Runge–Kutta method. Only when the Hamiltonian is separable as above, the PAVF method can then be a Runge–Kutta method if one adopt the same quadrature rule for both integrals, or a partitioned Runge–Kutta method if one use different quadrature rules to replace the integrals.

Remark 2.4. For the non-constant structure such as the case when $S_{2d} = S_{2d}(p,q)$ which is dependent on the solutions, we will not straightly apply the PAVF method on the entire vector field. Instead, we can fix the solutions in S_{2d} at time level t_n for a simple example, resulting the following PAVF-like scheme

$$\frac{1}{\tau}\begin{pmatrix} p^{n+1}-p^n \\ q^{n+1}-q^n \end{pmatrix} = S_{2d}(p^n,q^n)\begin{pmatrix} \int_0^1 H_p(\xi p^{n+1}+(1-\xi)p^n, q^n)\mathrm{d}\xi \\ \int_0^1 H_q(p^{n+1}, \xi q^{n+1}+(1-\xi)q^n)\mathrm{d}\xi \end{pmatrix},$$

which can also preserve the Hamiltonian based on the proof in Theorem 2.1. For concrete problems, one can choose a better approximation of $S_{2d}(p,q)$ for the sake of improving the computational efficiency.

We denote the PAVF method (2.2) as Φ_τ, then its adjoint method Φ_τ^* can be obtained as follows

$$\frac{1}{\tau}\begin{pmatrix} p^{n+1}-p^n \\ q^{n+1}-q^n \end{pmatrix} = S_{2d}\begin{pmatrix} \int_0^1 H_p(\xi p^{n+1}+(1-\xi)p^n, q^{n+1})\mathrm{d}\xi \\ \int_0^1 H_q(p^n, \xi q^{n+1}+(1-\xi)q^n)\mathrm{d}\xi \end{pmatrix}. \tag{2.3}$$

Obviously, the adjoint method Φ_τ^* (2.3) belongs to the PAVF method, only with a reversed path order to that of Φ_τ. Consequently, the adjoint method (2.3) can also exactly preserve the Hamiltonian $H(z)$ and possess all the properties of the PAVF method.

In conjunction with the adjoint PAVF method, we can define the following PAVF composition (PAVF-C) method

$$\Psi_\tau := \Phi^*_{\frac{\tau}{2}} \circ \Phi_{\frac{\tau}{2}}, \tag{2.4}$$

and partitioned AVF plus (PAVF-P) method

$$\hat{\Psi}_\tau := \frac{1}{2}(\Phi_\tau^* + \Phi_\tau), \tag{2.5}$$

respectively.

Theorem 2.2. *The PAVF-C method Ψ_τ (2.4) and PAVF-P method $\hat{\Psi}_\tau$ (2.5) are both second-order methods which can conserve the energy of the Hamiltonian system (2.6) exactly.*

Proof. It is clear that these two methods are both symmetric and thereby of second-order accuracy. Using the fact that either the PAVF method or its adjoint can exactly preserve the same Hamiltonian, the operators of their composition (2.4) and plus (2.5) still inherit this property that ends the proof. □

Next, we consider a more general case of the Hamiltonian system (1.1) with $m = \tilde{m}d$ which can come from the semi-discretization of Hamiltonian PDEs. The corresponding grouping strategy is the same as that in Remark 2.2 and for convenience we just take $z = (\tilde{z}_1, \tilde{z}_2, ..., \tilde{z}_{\tilde{m}-1}, \tilde{z}_{\tilde{m}})$ where $\tilde{z}_k \in \mathbb{R}^d$, $k = 1, 2, ..., \tilde{m}$. Under this circumstance, the Hamiltonian system (1.1) becomes

$$\begin{pmatrix} \dot{\tilde{z}}_1 \\ \dot{\tilde{z}}_2 \\ \vdots \\ \dot{\tilde{z}}_{\tilde{m}-1} \\ \dot{\tilde{z}}_{\tilde{m}} \end{pmatrix} = S_{\tilde{m}d}\begin{pmatrix} H_{\tilde{z}_1}(\tilde{z}_1, \tilde{z}_2, ..., \tilde{z}_{\tilde{m}-1}, \tilde{z}_{\tilde{m}}) \\ H_{\tilde{z}_2}(\tilde{z}_1, \tilde{z}_2, ..., \tilde{z}_{\tilde{m}-1}, \tilde{z}_{\tilde{m}}) \\ \vdots \\ H_{\tilde{z}_{\tilde{m}-1}}(\tilde{z}_1, \tilde{z}_2, ..., \tilde{z}_{\tilde{m}-1}, \tilde{z}_{\tilde{m}}) \\ H_{\tilde{z}_{\tilde{m}}}(\tilde{z}_1, \tilde{z}_2, ..., \tilde{z}_{\tilde{m}-1}, \tilde{z}_{\tilde{m}}) \end{pmatrix}. \tag{2.6}$$

For this general case, the PAVF method is defined by

$$\frac{1}{\tau}\begin{pmatrix} \tilde{z}_1^{n+1}-\tilde{z}_1^n \\ \tilde{z}_2^{n+1}-\tilde{z}_2^n \\ \vdots \\ \tilde{z}_{\tilde{m}-1}^{n+1}-\tilde{z}_{\tilde{m}-1}^n \\ \tilde{z}_{\tilde{m}}^{n+1}-\tilde{z}_{\tilde{m}}^n \end{pmatrix} = S_{\tilde{m}d}\begin{pmatrix} \int_0^1 H_{\tilde{z}_1}(\xi\tilde{z}_1^{n+1}+(1-\xi)\tilde{z}_1^n, \tilde{z}_2^n, ..., \tilde{z}_{\tilde{m}-1}^n, \tilde{z}_{\tilde{m}}^n)\mathrm{d}\xi \\ \int_0^1 H_{\tilde{z}_2}(\tilde{z}_1^{n+1}, \xi\tilde{z}_2^{n+1}+(1-\xi)\tilde{z}_2^n, ..., \tilde{z}_{\tilde{m}-1}^n, \tilde{z}_{\tilde{m}}^n)\mathrm{d}\xi \\ \vdots \\ \int_0^1 H_{\tilde{z}_{\tilde{m}-1}}(\tilde{z}_1^{n+1}, \tilde{z}_2^{n+1}, ..., \xi\tilde{z}_{\tilde{m}-1}^{n+1}+(1-\xi)\tilde{z}_{\tilde{m}-1}^n, z_{\tilde{m}}^n)\mathrm{d}\xi \\ \int_0^1 H_{\tilde{z}_{\tilde{m}}}(\tilde{z}_1^{n+1}, \tilde{z}_2^{n+1}, ..., \tilde{z}_{\tilde{m}-1}^{n+1}, \xi\tilde{z}_{\tilde{m}}^{n+1}+(1-\xi)\tilde{z}_{\tilde{m}}^n)\mathrm{d}\xi \end{pmatrix}. \tag{2.7}$$

Theorem 2.3. *The PAVF method (2.7) preserves the Hamiltonian $H(z)$ of the general system (2.6) exactly, and satisfies*

$$\frac{1}{\tau}(H(z^{n+1}) - H(z^n)) = 0.$$

Proof. In analogy to the proof of above theorem (2.1), we can get

$$0 = \frac{1}{\tau}\sum_{k=1}^{\tilde{m}}\Big[\int_0^1 H_{\tilde{z}_k}(\tilde{z}_1^{n+1}, ..., \tilde{z}_{k-1}^{n+1}, \xi\tilde{z}_k^{n+1}+(1-\xi)\tilde{z}_k^n, \tilde{z}_{k+1}^n, ..., \tilde{z}_{\tilde{m}}^n)d\xi\Big]^T(\tilde{z}_k^{n+1}-\tilde{z}_k^n)$$

$$=\frac{1}{\tau}\sum_{k=1}^{\tilde{m}}(H(\tilde{z}_1^{n+1},...,\tilde{z}_{k-1}^{n+1},\tilde{z}_k^{n+1},\tilde{z}_{k+1}^{n},...,\tilde{z}_{\tilde{m}}^{n})-H(\tilde{z}_1^{n+1},...,\tilde{z}_{k-1}^{n+1},\tilde{z}_k^{n},\tilde{z}_{k+1}^{n},...,\tilde{z}_{m}^{n}))$$
$$=\frac{1}{\tau}(H(\tilde{z}_1^{n+1},\tilde{z}_2^{n+1},\tilde{z}_3^{n+1},...,\tilde{z}_{\tilde{m}}^{n+1})-H(\tilde{z}_1^{n},\tilde{z}_2^{n},\tilde{z}_3^{n},...,\tilde{z}_{\tilde{m}}^{n})).\quad\square$$

We can also derive the its adjoint scheme as

$$\frac{1}{\tau}\begin{pmatrix}\tilde{z}_1^{n+1}-\tilde{z}_1^{n}\\ \tilde{z}_2^{n+1}-\tilde{z}_2^{n}\\ \vdots\\ \tilde{z}_{\tilde{m}-1}^{n+1}-\tilde{z}_{\tilde{m}-1}^{n}\\ \tilde{z}_{\tilde{m}}^{n+1}-\tilde{z}_{\tilde{m}}^{n}\end{pmatrix}=S_{\tilde{m}d}\begin{pmatrix}\int_0^1 H_{\tilde{z}_1}(\xi\tilde{z}_1^{n+1}+(1-\xi)\tilde{z}_1^{n},\tilde{z}_2^{n+1},...,\tilde{z}_{\tilde{m}-1}^{n+1},\tilde{z}_{\tilde{m}}^{n+1})\mathrm{d}\xi\\ \int_0^1 H_{\tilde{z}_2}(\tilde{z}_1^{n},\xi\tilde{z}_2^{n+1}+(1-\xi)\tilde{z}_2^{n},...,\tilde{z}_{\tilde{m}-1}^{n+1},\tilde{z}_{\tilde{m}}^{n+1})\mathrm{d}\xi\\ \vdots\\ \int_0^1 H_{\tilde{z}_{\tilde{m}-1}}(\tilde{z}_1^{n},\tilde{z}_2^{n},...,\xi\tilde{z}_{\tilde{m}-1}^{n+1}+(1-\xi)\tilde{z}_{\tilde{m}-1}^{n},z_{\tilde{m}}^{n+1})\mathrm{d}\xi\\ \int_0^1 H_{\tilde{z}_{\tilde{m}}}(\tilde{z}_1^{n},\tilde{z}_2^{n},...,\tilde{z}_{\tilde{m}-1}^{n},\xi\tilde{z}_{\tilde{m}}^{n+1}+(1-\xi)\tilde{z}_{\tilde{m}}^{n})\mathrm{d}\xi\end{pmatrix}.\tag{2.8}$$

Thereafter, the PAVF-C and PAVF-P methods for general Hamiltonian system can be obtained.

Notice that the proposed PAVF method is a special case of the discrete gradient method [10], which generally has the form

$$\frac{z^{n+1}-z^{n}}{\tau}=S_m\overline{\nabla}H(z^{n+1},z^{n})\tag{2.9}$$

for the system (1.1). However, there are various definitions of the discrete gradient $\overline{\nabla}H(z^{n+1},z^{n})$ [10]. One can choose the coordinate increment discrete gradient [19] as

$$\overline{\nabla}H(\bar{z},z):=\begin{pmatrix}\dfrac{H(\bar{z}_1,z_2,z_2,...,z_m)-H(z_1,z_2,z_3,...,z_m)}{\bar{z}_1-z_1}\\ \dfrac{H(\bar{z}_1,\bar{z}_2,z_3,...,z_m)-H(\bar{z}_1,z_2,z_3,...,z_m)}{\bar{z}_2-z_2}\\ \vdots\\ \dfrac{H(\bar{z}_1,...,\bar{z}_{m-2},\bar{z}_{m-1},z_m)-H(\bar{z}_1,...,\bar{z}_{m-2},z_{m-1},z_m)}{\bar{z}_{m-1}-z_{m-1}}\\ \dfrac{H(\bar{z}_1,...,\bar{z}_{m-2},\bar{z}_{m-1},\bar{z}_m)-H(\bar{z}_1,...,\bar{z}_{m-2},\bar{z}_{m-1},z_m)}{\bar{z}_m-z_m}\end{pmatrix},\tag{2.10}$$

with the notation $\bar{z}=z^{n+1}$, $z=z^{n}$, which can be further regarded as vector of the means of the tangential components of ∇H along each of the m segments of the path joining $\bar{z}$ and z by incrementing the coordinates one at a time [10], that is

$$(\overline{\nabla}H(\bar{z},z))_k=\int_0^1\frac{\partial H}{\partial z_k}(\bar{z}_1,...,\bar{z}_{k-1},\xi\bar{z}_k+(1-\xi)z_k,z_{k+1},...,z_m)\mathrm{d}\xi.\tag{2.11}$$

The PAVF method is directly inspired by the discrete gradient method (2.10) and its equivalent form (2.11). The major difference is that instead of dividing the path along z to $\bar{z}$ into m segments, we first group the components according to the cross-product terms in the gradient of the Hamiltonian and then apply the processes of incrementing the group one at a time. As a consequence, the choices of the grouping strategy are flexible, which can lead to more efficient energy-preserving schemes.

In the next section, we will apply the class of PAVF methods on both ODEs and PDEs, and construct concrete energy-preserving schemes.

3. Numerical examples

3.1. Hénon–Heiles system

Consider the Hénon–Heiles system

$$\dot{z}=J\nabla H(z),\quad H(z)=\frac{1}{2}(q_1^2+q_2^2+p_1^2+p_2^2)+q_1^2q_2-\frac{1}{3}q_2^3,\tag{3.1}$$

where $z=(q_1,q_2,p_1,p_2)^T$ and $J=\begin{pmatrix}0 & I\\ -I & 0\end{pmatrix}$ with I a 2×2 identity matrix. This model was created for describing stellar motion, followed for a very long time, inside the gravitational potential of a galaxy with cylindrical [6]. The Hénon–Heiles

system (3.1) has a finite energy of escape H_{esc} which is equal to 1/6. For values of energy $H < H_{esc}$, the equipotential curves of the system are close thus making escape impossible. However, for energy greater than H_{esc}, the equipotential curves open and three exit channels appear through which the test particles may escape to infinity [20].

3.1.1. Derivation of the partitioned AVF schemes

In contrast, we first present the conventional second-order AVF method (1.2) for the Hénon–Heiles system which can be derived directly based on the formula (1.2) as follows

$$\begin{aligned}
&\frac{1}{\tau}(q_1^{n+1}-q_1^n)=\frac{1}{2}(p_1^{n+1}+p_1^n),\\
&\frac{1}{\tau}(q_2^{n+1}-q_2^n)=\frac{1}{2}(p_2^{n+1}+p_2^n),\\
&\frac{1}{\tau}(p_1^{n+1}-p_1^n)=-(\frac{1}{2}(q_1^{n+1}+q_1^n)+\frac{1}{3}(q_1^{n+1}q_2^{n+1}+4q_1^{n+\frac{1}{2}}q_2^{n+\frac{1}{2}}+q_1^nq_2^n)),\\
&\frac{1}{\tau}(p_2^{n+1}-p_2^n)=-\frac{1}{2}(q_2^{n+1}+q_2^n)+\frac{1}{3}((q_2^{n+1})^2+q_2^{n+1}q_2^n+(q_2^n)^2-(q_1^{n+1})^2-q_1^{n+1}q_1^n-(q_1^n)^2).
\end{aligned}\tag{3.2}$$

Notice that in this example, the PAVF method for the system (3.1) is actually equivalent to the discrete gradient method (2.10) with the corresponding discrete gradient defined by (2.11), which is a special case from the proposed general PAVF method (2.6) when $d=1, m=4$. Then the PAVF method for the Hénon–Heiles system (3.1) reads

$$\frac{1}{\tau}\begin{pmatrix} q_1^{n+1}-q_1^n\\ q_2^{n+1}-q_2^n\\ p_1^{n+1}-p_1^n\\ p_2^{n+1}-p_2^n\end{pmatrix}=J\begin{pmatrix} \int_0^1 H_{q_1}(\xi q_1^{n+1}+(1-\xi)q_1^n,q_2^n,p_1^n,p_2^n)\mathrm{d}\xi\\ \int_0^1 H_{q_2}(q_1^{n+1},\xi q_2^{n+1}+(1-\xi)q_2^n,p_1^n,p_2^n)\mathrm{d}\xi\\ \int_0^1 H_{p_1}(q_1^{n+1},q_2^{n+1},\xi p_1^{n+1}+(1-\xi)p_1^n,p_2^n)\mathrm{d}\xi\\ \int_0^1 H_{p_2}(q_1^{n+1},q_2^{n+1},p_1^{n+1},\xi p_2^{n+1}+(1-\xi)p_2^n)\mathrm{d}\xi\end{pmatrix},\tag{3.3}$$

which can be further simplified as

$$\begin{aligned}
&\frac{1}{\tau}(q_1^{n+1}-q_1^n)=\frac{1}{2}(p_1^{n+1}+p_1^n),\\
&\frac{1}{\tau}(q_2^{n+1}-q_2^n)=\frac{1}{2}(p_2^{n+1}+p_2^n),\\
&\frac{1}{\tau}(p_1^{n+1}-p_1^n)=-(\frac{1}{2}(q_1^{n+1}+q_1^n)+(q_1^{n+1}+q_1^n)q_2^n),\\
&\frac{1}{\tau}(p_2^{n+1}-p_2^n)=-(\frac{1}{2}(q_2^{n+1}+q_2^n)+(q_1^{n+1})^2)+\frac{1}{3}((q_2^{n+1})^2+q_2^{n+1}q_2^n+(q_2^n)^2).
\end{aligned}\tag{3.4}$$

It is clear that the PAVF method (3.4) is simpler than the original one (3.2) at first glance. Furthermore, we can find the former scheme is semi-implicit, that is given $(q_1^n,q_2^n,p_1^n,p_2^n)$ the values q_1^{n+1} and p_1^{n+1} can be calculated from the first and third equations of (3.4) explicitly, leaving only q_2^{n+1}, p_2^{n+1} being solved by numerical iterations. In contrast, the conventional AVF method (3.2) has to run an iteration involving all the variable $(q_1^{n+1},q_2^{n+1},p_1^{n+1},p_2^{n+1})$ which double the computational scale of the PAVF method (3.4). Therefore, the PAVF method is apparently more effective than the AVF method.

In conjunction with the adjoint method of (3.4) we can derive the PAVF-C method

$$\begin{aligned}
&\frac{2}{\tau}(q_1^*-q_1^n)=\frac{1}{2}(p_1^*+p_1^n),\\
&\frac{2}{\tau}(q_2^*-q_2^n)=\frac{1}{2}(p_2^*+p_2^n),\\
&\frac{2}{\tau}(p_1^*-p_1^n)=-(\frac{1}{2}(q_1^*+q_1^n)+(q_1^*+q_1^n)q_2^n),\\
&\frac{2}{\tau}(p_2^*-p_2^n)=-(\frac{1}{2}(q_2^*+q_2^n)+(q_1^*)^2)+\frac{1}{3}((q_2^*)^2+q_2^*q_2^n+(q_2^n)^2),\\
&\frac{2}{\tau}(q_1^{n+1}-q_1^*)=\frac{1}{2}(p_1^{n+1}+p_1^*),\\
&\frac{2}{\tau}(q_2^{n+1}-q_2^*)=\frac{1}{2}(p_2^{n+1}+p_2^*),\\
&\frac{2}{\tau}(p_1^{n+1}-p_1^*)=-(\frac{1}{2}(q_1^{n+1}+q_1^*)+(q_1^{n+1}+q_1^*)q_2^{n+1}),\\
&\frac{2}{\tau}(p_2^{n+1}-p_2^*)=-(\frac{1}{2}(q_2^{n+1}+q_2^*)+(q_1^*)^2)+\frac{1}{3}((q_2^{n+1})^2+q_2^{n+1}q_2^*+(q_2^*)^2),
\end{aligned}\tag{3.5}$$

and the corresponding PAVF-P method

$$\begin{aligned}
&\frac{1}{\tau}(q_1^{n+1}-q_1^n)=\frac{1}{2}(p_1^{n+1}+p_1^n),\\
&\frac{1}{\tau}(q_2^{n+1}-q_2^n)=\frac{1}{2}(p_2^{n+1}+p_2^n),\\
&\frac{1}{\tau}(p_1^{n+1}-p_1^n)=-\frac{1}{2}(q_1^{n+1}+q_1^n+(q_1^{n+1}+q_1^n)(q_2^{n+1}+q_2^n)),\\
&\frac{1}{\tau}(p_2^{n+1}-p_2^n)=-\frac{1}{2}(q_2^{n+1}+q_2^n+(q_1^{n+1})^2+(q_1^n)^2)+\frac{1}{3}((q_2^{n+1})^2+q_2^{n+1}q_2^n+(q_2^n)^2),
\end{aligned}\tag{3.6}$$

for the Hénon–Heiles system (3.1). As aforementioned, both the two methods are energy-preserving and of second order accuracy. In addition, the PAVF-C method can inherit the semi-implicit property which however is no long satisfied by the PAVF-P method in view of the third equation in (3.6).

3.1.2. Numerical experiments

In the following experiments, we will test two classic orbits of the Hénon–Heiles system (3.1): (i) chaotic orbits ($H^0 = 1/6$), (ii) box orbits ($H^0 = 0.02$) with initial conditions $(q_1, q_2, p_2) = (0.1, -0.5, 0)$ and $(0, -0.082, 0)$. The leaving p_1 is found from the energy function (3.1). We solve the two cases by the AVF method (3.2), the PAVF method (3.4), the PAVF-C method (3.5) and the PAVF-P method (3.6), respectively. The temporal increment is always set to $\tau = 0.2$. The relative energy error is defined by

$$RH^n = \left|(H^n - H^0)/H^0\right|,$$

where H^n denotes the Hamiltonian at $t = t^n$.

In Fig. 1 it is clear that under the critical energy 1/6 all the methods can ensure the numerical trajectory never escape the triangle for any value of t and present the chaotic orbits as expected. While for the second case $H^0 = 0.02$, the four methods can also recurrence the box orbits in Fig. 2. Besides the result from the PAVF method, the inner shape of orbits all exhibits like an equilateral triangle. While the associate shape of the PAVF method suffers a little deformation which is probably caused by its lower accuracy. This can be also conformed from the corresponding Poincaré cuts in Fig. 3. Furthermore, we find that the density between the orbits are very relied on the temporal increment. If we set $\tau = 0.21$, the orbits of the PAVF-P method are very similar to that of the PAVF-C method. In Fig. 4, we present the corresponding errors in the discrete energy of all methods which uniformly reach the machine accuracy but with a linear growth mainly caused by the numerical iteration. Although the complexity of the four schemes is clear from the above analysis, due to the restriction of the computing scale of the Hénon–Heiles system, the difference of the computational cost is very slight even though we set the end time as 2×10^5. Therefore, we will demonstrate this superiority of the PAVF method in the following PDE cases.

3.2. Klein–Gordon–Schrödinger equation

We consider the following Klein–Gordon–Schrödinger (KGS) equation:

$$\begin{aligned}
&i\varphi_t + \frac{1}{2}\varphi_{xx} + u\varphi = 0,\\
&u_{tt} - u_{xx} + u - |\varphi|^2 = 0,
\end{aligned}\qquad x \in (x_L, x_R),\ t > 0,\tag{3.7}$$

which describes a system of conserved scalar nucleons interacting with neutral scalar Mesons coupled with Yukawa interaction, where $\phi(x,t)$ represents a complex scalar nucleon field, $u(x,t)$ a real scalar meson field [21].

The conservation of energy is a crucial property for the KGS equations. Let $\varphi = q + pi$ and $v = \frac{1}{2}u_t$. We can rewrite (3.7) as a first-order system

$$\begin{aligned}
&u_t = 2v,\\
&v_t = \frac{1}{2}(u_{xx} - u + (p^2 + q^2)),\\
&p_t = \frac{1}{2}q_{xx} + uq,\\
&q_t = -\frac{1}{2}p_{xx} - up.
\end{aligned}\tag{3.8}$$

Under homogeneous Dirichlet boundary conditions

$$\begin{aligned}
&p(x_L,t) = p(x_R,t) = 0, \quad q(x_L,t) = q(x_R,t) = 0,\\
&u(x_L,t) = u(x_R,t) = 0, \quad v(x_L,t) = v(x_R,t) = 0,
\end{aligned}$$

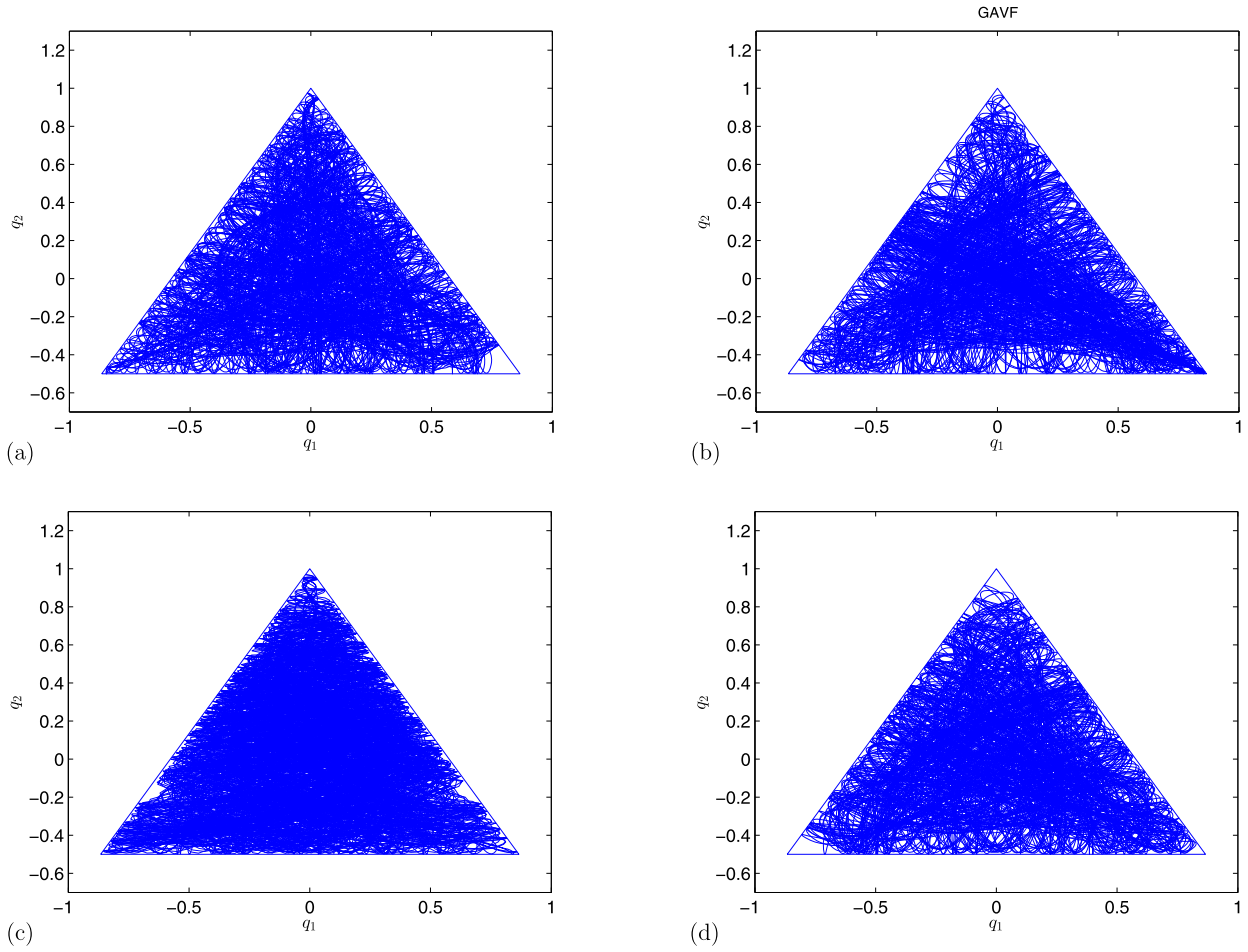

Fig. 1. Chaotic orbits of the four energy-preserving methods for the Hénon–Heiles system till $t = 2000$. (a): The AVF method; (b): The PAVF method; (c): The PAVF-C method; (d): The PAVF-P method.

the above system (3.8) can be comprised to an infinite-dimensional Hamiltonian system

$$\frac{dz}{dt} = S\frac{\delta \mathcal{H}(z)}{\delta z}, \tag{3.9}$$

where $z = (u, v, p, q)^T$, $S = \begin{bmatrix} 0 & 1 & 0 & 0 \\ -1 & 0 & 0 & 0 \\ 0 & 0 & 0 & -1 \\ 0 & 0 & 1 & 0 \end{bmatrix}$, and the Hamiltonian functional is defined by

$$H(z) = \int_{x_L}^{x_R} \frac{1}{4}\left[p_x^2 + q_x^2 + u^2 + u_x^2 + 4v^2 - 2u(p^2 + q^2)\right] \mathrm{d}x.$$

Besides the energy conservation law $H(z(t)) = H(z(0))$, the KGS system further obeys the mass conservation law

$$M(z(t)) = \int_{x_L}^{x_R} (p^2 + q^2) dx = M(z(0)).$$

3.2.1. Derivation of the partitioned AVF schemes

Notice that in the current work we mainly focus on the partitioned AVF methods for Hamiltonian systems, therefore, we just take the conventional spatial discretization for illustration. Hereafter, we choose the second-order central difference operator to approximate the spatial derivatives in (3.8). To present the concrete numerical schemes, we first introduce some notations.

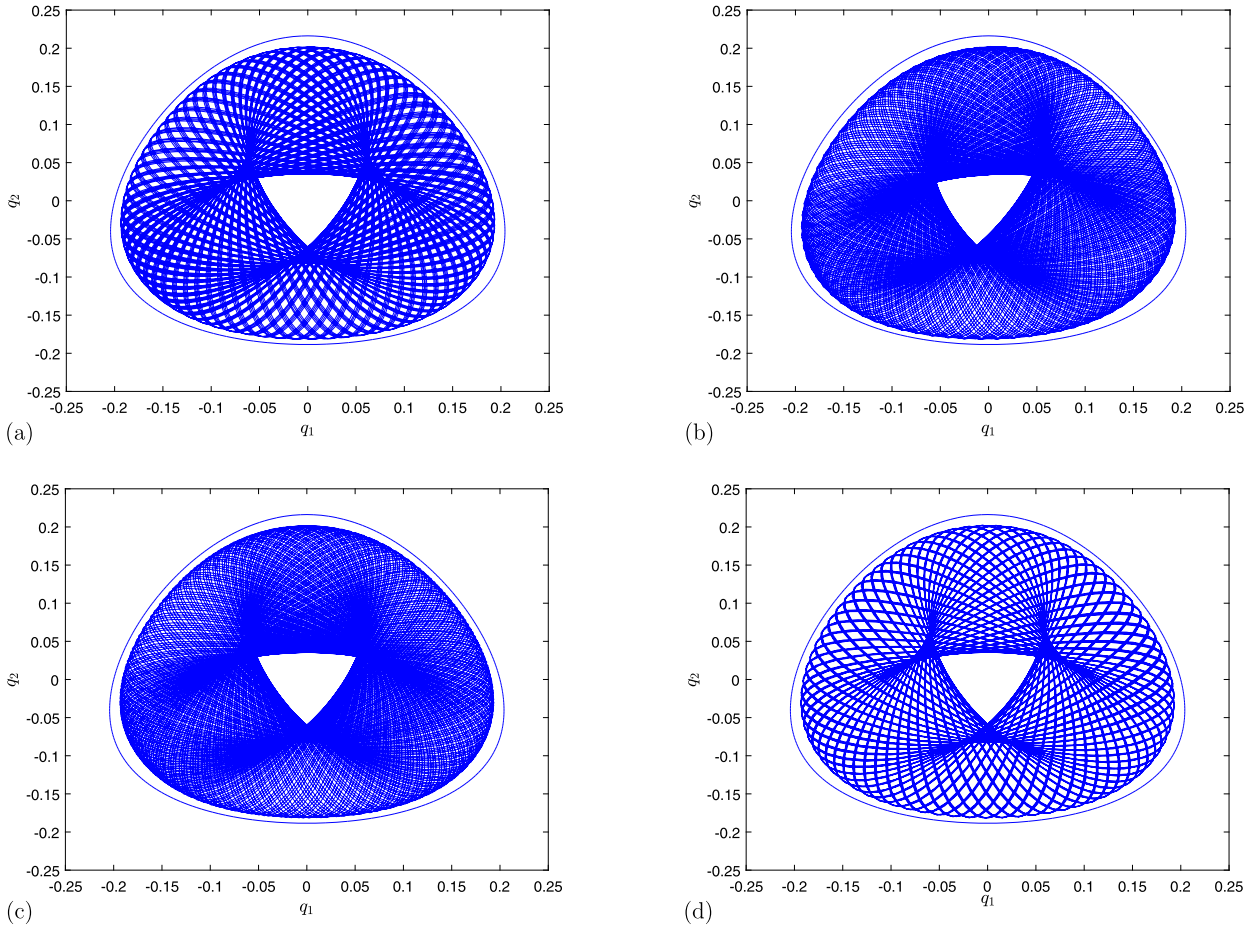

Fig. 2. Box orbits of the four energy-preserving methods for the Hénon–Heiles system till $t = 1000$. (a): The AVF method; (b): The PAVF method; (c): The PAVF-C method; (d): The PAVF-P method.

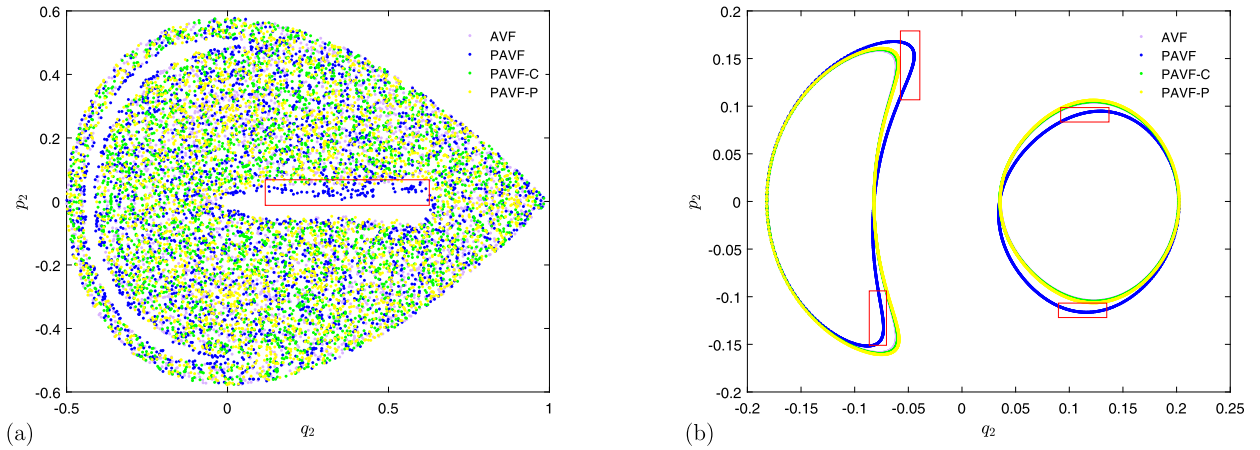

Fig. 3. Poincaré cuts for the four numerical method (a): $H^0 = 1/6$; (b): $H^0 = 0.02$. The blue dots in red boxes show a little drift of obits produced by the first-order PAVF method. (For interpretation of the colors in the figure(s), the reader is referred to the web version of this article.)

The spatial-temporal domain is discretized as follows: $t_n = n\tau$, for $n = 0, 1, ...,$ and $x_j = x_L + jh$, for $j = 0, 1, ..., J$ where $h = L/J$ and τ are the spatial and temporal steps. Let $(u_j^n, v_j^n, p_j^n, q_j^n)$ be the numerical approximations to the exact solutions $(u(x,t), v(x,t), p(x,t), q(x,t))$ at the grid point (x_j, t_n). The corresponding vector forms at any time level are then denoted

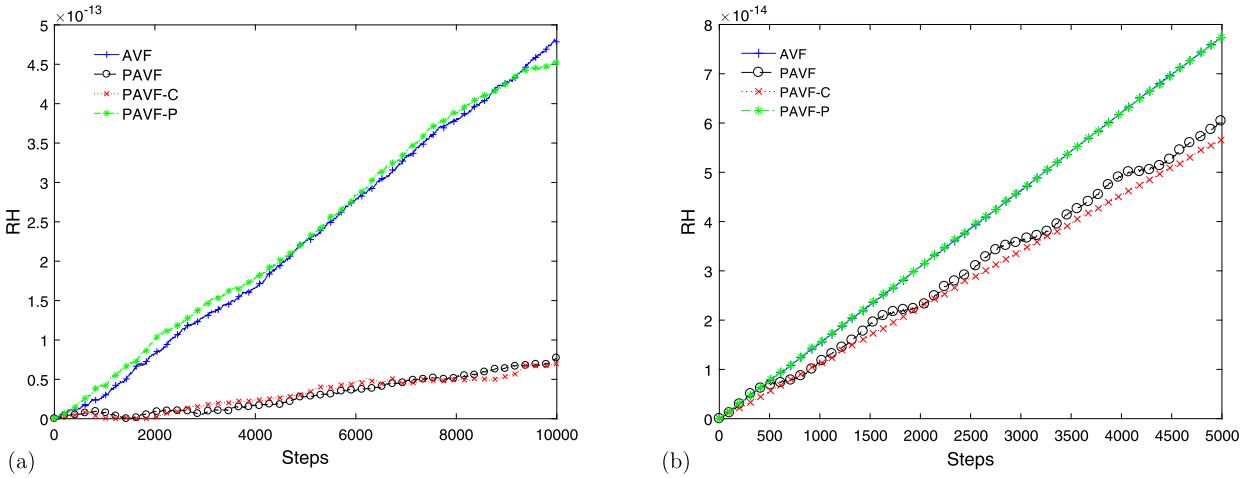

Fig. 4. Relative energy error of the four energy-preserving methods for the Hénon–Heiles system with chaotic orbits (a) and box orbits (b).

by

$$U = (u_0, u_1, \ldots, u_J)^T, \quad V = (v_0, v_1, \ldots, v_J)^T,$$
$$P = (p_0, p_1, \ldots, p_J)^T, \quad Q = (q_0, q_1, \ldots, q_J)^T.$$

With these notations, we can define the inner product as well as norms of vectors:

$$(U, V) = h \sum_{j=0}^{J} u_j \bar{v}_j, \quad \|U\|_J = (U, U)^{\frac{1}{2}}, \quad \|U\|_\infty = \max_j |u_j|.$$

The semi-discretization of the KGS equation (3.8) by the central difference scheme can be written as

$$\begin{aligned} U_t &= 2V, \\ V_t &= \frac{1}{2} DU - \frac{1}{2} U + \frac{1}{2}(P^2 + Q^2), \\ P_t &= \frac{1}{2} DQ + U \cdot Q, \\ Q_t &= -\frac{1}{2} DP - U \cdot P, \end{aligned} \tag{3.10}$$

where D represents the central differentiation matrix, and the operation $P^2 = P \cdot P$. Here, '$\cdot$' means the point multiplication between vectors, that is, $P \cdot Q = (p_0 q_0, p_1 q_1, \ldots, p_J q_J)^T$. In analogy to the continuous case, we can also transform the system (3.10) back to a finite-dimensional canonical Hamiltonian form

$$\frac{dZ}{dt} = f(Z) = S \nabla H(Z), \tag{3.11}$$

where $Z = (U^T, V^T, P^T, Q^T)^T$, $S = \begin{bmatrix} 0 & I & 0 & 0 \\ -I & 0 & 0 & 0 \\ 0 & 0 & 0 & -I \\ 0 & 0 & I & 0 \end{bmatrix}$, and the discrete Hamiltonian is defined by

$$H(Z) = \frac{1}{4}\left(-P^T DP - Q^T DQ - U^T DU + U^T U + 4V^T V - 2U^T\left(P^2 + Q^2\right)\right).$$

From system (3.11), we can derive the semi-discrete energy conservation law

$$\frac{dH(Z(t))}{dt} = \nabla H(Z)^T f(Z) = \nabla H(Z)^T S \nabla H(Z) = 0,$$

and letting $M(Z) = \|P\|_J^2 + \|Q\|_J^2$, we also have the semi-discrete mass conservation law

$$\frac{dM(Z)}{dt} = 2h\left(\frac{1}{2} P^T DQ - \frac{1}{2} Q^T DP + P^T (U \cdot Q) - Q^T (U \cdot P)\right) = 0.$$

Hence, the flow of the semi-discrete system (3.10) preserves both the total energy $H(Z)$ and mass $M(Z)$ exactly.

The following part is devoted to the construction of the partitioned AVF methods (2.7), (2.4) and (2.5) for the KGS equation (3.7). For comparison we also present the original second-order AVF scheme

$$\begin{aligned}
&\delta_t^+ U^n = V^n + V^{n+1},\\
&\delta_t^+ V^n = \frac{1}{2}(DU^{n+\frac{1}{2}} - U^{n+\frac{1}{2}}) + \frac{1}{12}((P^{n+1})^2 + 4(P^{n+\frac{1}{2}})^2 + (P^n)^2 + (Q^{n+1})^2 + 4(Q^{n+\frac{1}{2}})^2 + (Q^n)^2),\\
&\delta_t^+ P^n = \frac{1}{2}DQ^{n+\frac{1}{2}} + \frac{1}{6}(U^{n+1}\cdot Q^{n+1} + 4U^{n+\frac{1}{2}}\cdot Q^{n+\frac{1}{2}} + U^n\cdot Q^n),\\
&\delta_t^+ Q^n = -\frac{1}{2}DP^{n+\frac{1}{2}} - \frac{1}{6}(U^{n+1}\cdot P^{n+1} + 4U^{n+\frac{1}{2}}\cdot P^{n+\frac{1}{2}} + U^n\cdot P^n),
\end{aligned} \tag{3.12}$$

where δ_t^+ is the standard forward differential operator. Obviously, the AVF method for the KGS equation is a fully implicit scheme but with the energy-preserving property.

Next, we introduce our partitioned AVF methods. Under this circumstance, the dimension parameters in (2.6) are set to $\tilde{m} = 4$ and $d = J + 1$. Then the corresponding PAVF scheme yields

$$\begin{aligned}
&\delta_t^+ U^n = \int_0^1 H_V(U^{n+1}, \xi V^{n+1} + (1-\xi)V^n, P^n, Q^n)d\xi,\\
&\delta_t^+ V^n = -\int_0^1 H_U(\xi U^{n+1} + (1-\xi)U^n, V^n, P^n, Q^n)d\xi,\\
&\delta_t^+ Q^n = -\int_0^1 H_Q(U^{n+1}, V^{n+1}, P^{n+1}, \xi Q^{n+1} + (1-\xi)Q^n)d\xi,\\
&\delta_t^+ Q^n = \int_0^1 H_P(U^{n+1}, V^{n+1}, \xi P^{n+1} + (1-\xi)P^n, Q^n)d\xi,
\end{aligned} \tag{3.13}$$

which can be further integrated as

$$\begin{aligned}
&\delta_t^+ U^n = V^n + V^{n+1},\\
&\delta_t^+ V^n = \frac{1}{2}(DU^{n+\frac{1}{2}} - U^{n+\frac{1}{2}} + (P^n)^2 + (Q^n)^2),\\
&\delta_t^+ P^n = \frac{1}{2}DQ^{n+\frac{1}{2}} + U^{n+1}\cdot Q^{n+\frac{1}{2}},\\
&\delta_t^+ Q^n = -\frac{1}{2}DP^{n+\frac{1}{2}} - U^{n+1}\cdot P^{n+\frac{1}{2}}.
\end{aligned} \tag{3.14}$$

Apparently, the PAVF scheme (3.14) is simpler than the AVF scheme (3.12) that just requires to solve two sets of linear algebraic equations in contrast to apply numerical iterations for the entire system.

Theorem 3.1. *Beside the energy conservation, the PAVF method (3.14) is also mass conservative. That is, its solution satisfies the following conservation laws*

$$M(U^n, V^n, P^n, Q^n) = M(U^0, V^0, P^0, Q^0), \quad \forall\, n = 1, 2, \dots.$$

Proof. Taking the discrete inner products of the last two equations in (3.14) with $P^{n+1} + P^n$ and $Q^{n+1} + Q^n$ respectively, we obtain

$$\frac{h}{\tau}(P^{n+1} + P^n)^T(P^{n+1} - P^n) = h(P^{n+1} + P^n)^T(\frac{1}{2}DQ^{n+\frac{1}{2}} + U^{n+1}\cdot Q^{n+\frac{1}{2}}), \tag{3.15}$$

and

$$\frac{h}{\tau}(Q^{n+1} + Q^n)^T(Q^{n+1} - Q^n) = h(Q^{n+1} + Q^n)^T(-\frac{1}{2}DP^{n+\frac{1}{2}} - U^{n+1}\cdot P^{n+\frac{1}{2}}). \tag{3.16}$$

Summing (3.15) and (3.16) together, we get the mass conservation law

$$\frac{1}{\tau}\left(\|P^{n+1}\|_J^2 + \|Q^{n+1}\|_J^2 - \|P^n\|_J^2 - \|Q^n\|_J^2\right) = 0. \quad \square \tag{3.17}$$

Remark 3.1. Note that the standard AVF method (3.12) does not possess the additional mass conservation law while the PAVF method has for the Klein–Gordon–Schrödinger equation.

To derive the second-order partitioned AVF methods, including the PAVF-C and PAVF-P methods, we first present the adjoint of the PAVF scheme (3.14) for the KGS equation:

$$\begin{aligned}
&\delta_t^+ U^n = V^n + V^{n+1},\\
&\delta_t^+ V^n = \frac{1}{2}(DU^{n+\frac{1}{2}} - U^{n+\frac{1}{2}} + (P^{n+1})^2 + (Q^{n+1})^2),\\
&\delta_t^+ P^n = \frac{1}{2}DQ^{n+\frac{1}{2}} + U^n \cdot Q^{n+\frac{1}{2}},\\
&\delta_t^+ Q^n = -\frac{1}{2}DP^{n+\frac{1}{2}} - U^n \cdot P^{n+\frac{1}{2}},
\end{aligned} \tag{3.18}$$

which can be similarly proved as an energy-mass-preserving method either. With the adjoint scheme (3.18), we can directly write down the corresponding PAVF-C scheme

$$\begin{aligned}
&\frac{1}{\tau}(U^* - U^n) = V^n + V^*,\\
&\frac{1}{\tau}(V^* - V^n) = \frac{1}{4}(D(U^* + U^n) - (U^* + U^n) + 2(P^n)^2 + 2(Q^n)^2),\\
&\frac{1}{\tau}(P^* - P^n) = \frac{1}{4}D(Q^* + Q^n) + \frac{1}{2}U^* \cdot (Q^* + Q^n),\\
&\frac{1}{\tau}(Q^* - Q^n) = -\frac{1}{4}D(P^* + P^n) - \frac{1}{2}U^* \cdot (P^* + P^n),\\
&\frac{1}{\tau}(U^{n+1} - U^*) = V^{n+1} + V^*,\\
&\frac{1}{\tau}(V^{n+1} - V^*) = \frac{1}{4}(D(U^* + U^{n+1}) - (U^* + U^{n+1}) + 2(P^{n+1})^2 + 2(Q^{n+1})^2),\\
&\frac{1}{\tau}(P^{n+1} - P^*) = \frac{1}{4}D(Q^* + Q^{n+1}) + \frac{1}{2}U^* \cdot (Q^* + Q^{n+1}),\\
&\frac{1}{\tau}(Q^{n+1} - Q^*) = -\frac{1}{4}D(P^* + P^{n+1}) - \frac{1}{2}U^* \cdot (P^* + P^{n+1}),
\end{aligned} \tag{3.19}$$

and the PAVF-P scheme

$$\begin{aligned}
&\delta_t^+ U^n = V^n + V^{n+1},\\
&\delta_t^+ V^n = \frac{1}{2}(DU^{n+\frac{1}{2}} - U^{n+\frac{1}{2}}) + \frac{1}{4}((P^n)^2 + (Q^n)^2 + (P^{n+1})^2 + (Q^{n+1})^2),\\
&\delta_t^+ P^n = \frac{1}{2}DQ^{n+\frac{1}{2}} + U^{n+\frac{1}{2}} \cdot Q^{n+\frac{1}{2}},\\
&\delta_t^+ Q^n = -\frac{1}{2}DP^{n+\frac{1}{2}} - U^{n+\frac{1}{2}} \cdot P^{n+\frac{1}{2}},
\end{aligned} \tag{3.20}$$

which both are symmetric methods of second-order accuracy and can also preserve the discrete energy and mass conservation laws.

Remark 3.2. In [22] authors also present two energy-preserving schemes for the KGS equation based on the coordinate increment discrete gradient method, which are equivalent to the adjoint and plus schemes here respectively. However, through the partitioned AVF strategy we can easily construct other energy-preserving schemes. Specifically, the resulting partitioned AVF composition scheme can not only conserve the discrete energy but also save computational time with second-order accuracy.

3.2.2. Numerical experiments

In this section, we consider the numerical results of the four energy-preserving methods for the KGS system (3.7). To measure the conservative properties, we define the relative energy and mass errors at $t = t_n$ as

$$RH^n = \left|(H^n - H^0)/H^0\right|, \quad RM^n = \left|(M^n - M^0)/M^0\right|.$$

Table 1
Temporal accuracy of the four energy-preserving methods with $h = 0.02$.

	τ	L^∞-error	order	L^2-error	order
AVF	1/10	1.15E–02	–	1.28E–02	–
	1/11	9.44E–03	2.04	1.05E–02	2.03
	1/12	7.90E–03	2.05	8.81E–03	2.04
	1/13	6.70E–03	2.06	7.48E–03	2.05
PAVF	1/10	1.06E–01	–	1.44E–02	–
	1/11	9.64E–02	0.98	1.27E–01	1.00
	1/12	8.85E–02	0.98	1.15E–01	1.00
	1/13	8.18E–02	0.98	1.06E–01	1.00
PAVF-C	1/10	4.42E–03	–	4.19E–03	–
	1/11	3.60E–03	2.14	3.42E–03	2.13
	1/12	2.98E–03	2.17	2.84E–03	2.15
	1/13	2.49E–03	2.21	2.38E–03	2.17
PAVF-P	1/10	9.60E–03	–	1.07E–02	–
	1/11	7.89E–03	2.06	8.82E–03	2.02
	1/12	6.59E–03	2.07	7.40E–03	2.03
	1/13	5.57E–03	2.09	6.29E–03	2.03

The discrete L^2-error and L^∞-error for solutions of the KGS equation are calculated by

$$L^2\text{-error}_n(h,\tau) = \|u(t_n) - U^n\|_J + \|v(t_n) - V^n\|_J + \|p(t_n) - P^n\|_J + \|q(t_n) - Q^n\|_J,$$
$$L^\infty\text{-error}_n(h,\tau) = \|u(t_n) - U^n\|_\infty + \|v(t_n) - V^n\|_\infty + \|p(t_n) - P^n\|_\infty + \|q(t_n) - Q^n\|_\infty.$$

The first example is about the propagation of one soliton, in which the initial conditions are taken as

$$\varphi(x,0) = \frac{3\sqrt{2}}{4\sqrt{1-c^2}}\operatorname{sech}^2\Big(\frac{1}{2\sqrt{1-c^2}}(x-x_0)\Big)\exp(icx),$$
$$u(x,0) = \frac{3}{4(1-c^2)}\operatorname{sech}^2\Big(\frac{1}{2\sqrt{1-c^2}}(x-x_0)\Big),$$
$$u_t(x,0) = \frac{3c}{4(1-c^2)^{3/2}}\operatorname{sech}^2\Big(\frac{1}{2\sqrt{1-c^2}}(x-x_0)\Big)\tanh\Big(\frac{1}{2\sqrt{1-c^2}}(x-x_0)\Big),$$

where $|c| < 1$ is the propagating velocity of the wave and x_0 is the initial phase. The exact solution is given by

$$\varphi(x,t) = \frac{3\sqrt{2}}{4\sqrt{1-c^2}}\operatorname{sech}^2\Big(\frac{1}{2\sqrt{1-c^2}}(x-ct-x_0)\Big)\exp\Big(i\big(cx+\frac{1-c^2+c^4}{2(1-c^2)}t\big)\Big),$$
$$u(x,t) = \frac{3}{4(1-c^2)}\operatorname{sech}^2\Big(\frac{1}{2\sqrt{1-c^2}}(x-ct-x_0)\Big).$$

We set the space interval $x \in [-10, 10]$ with parameters $c = -0.8$, $x_0 = 0$ and the homogeneous Dirichlet boundary conditions. In all numerical tests, we choose the fixed-point iterative algorithm as a nonlinear solver and the Gauss–Seidel iterative method as a linear solver. Table 1 and 2 give the temporal and spatial accuracy of the four energy-preserving methods. We can find that all the methods are both of second order in space and time except the PAVF method which is only first-order accuracy in time. The accuracy test validates the correctness of our methods.

To demonstrate the long-term behavior of the proposed methods, we enlarge the computational domain to $[-50, 50]$. The spatial and temporal steps are set to $h = 0.1$, $\tau = 0.05$. The initial phase is located at $x_0 = 20$. Fig. 5 presents the wave profiles of $|\Psi^n| = |Q^n + iP^n|$ and U^n from $t = 0$ to $t = 50$ which can be generated by all the four methods with almost same profiles. Moreover, in view of the relative errors in the energy and mass conservation laws (Fig. 6), we can find that the discrete energy can be preserved to round-off errors by any of the methods. However, the original AVF method can no long preserve the discrete mass conservation law even though the errors are always bounded during the time evolution. In contrast, the rest three partitioned AVF methods give an exact preservation of the discrete mass. In Table 3, we list the CPU time of the four methods with different spatial steps. Since the AVF method and the PAVF-P method are fully implicit, their computational costs are comparable but more than the PAVF method and the PAVF-C method which are only linearly implicit. Moreover, the CPU time of the PAVF-C method is much less than the twice of that of the PAVF method. To further compare the computational efficiency of the first-order PAVF method and the second-order PAVF-C method, Fig. 7 presents the numerical errors versus computational costs of these two methods on the domain of $[-10, 10]$ at $t = 1$, with different temporal steps $\Delta t = 0.2, 0.1, 0.05, 0.0025, 0.00125$ and corresponding spatial steps $h = 2/50, 2/100, 2/200, 2/400, 2/800$. It is clear that the PAVF-C method is more efficient than the PAVF method in consideration of both accuracy and computational cost.

Table 2
Spatial accuracy of the four energy-preserving methods with $\tau = 0.001$.

	h	L^∞-error	order	L^2-error	order
AVF	2/10	6.04E–02	–	6.50E–02	–
	2/15	2.64E–02	2.04	2.87E–02	2.02
	2/20	1.48E–02	2.01	1.61E–02	2.01
	2/25	9.47E–03	2.01	1.03E–02	2.01
PAVF	2/10	6.03E–02	–	6.49E–02	–
	2/15	2.63E–02	2.05	2.85E–02	2.02
	2/20	1.48E–02	2.00	1.60E–02	2.02
	2/25	9.42E–03	2.01	1.02E–02	2.01
PAVF-C	2/10	6.04E–02	–	6.50E–02	–
	2/15	2.64E–02	2.04	2.87E–02	2.02
	2/20	1.48E–02	2.01	1.61E–02	2.01
	2/25	9.47E–03	2.01	1.03E–02	2.01
PAVF-P	2/10	6.04E–02	–	6.50E–02	–
	2/15	2.64E–02	2.04	2.87E–02	2.02
	2/20	1.48E–02	2.01	1.61E–02	2.01
	2/25	9.47E–03	2.01	1.03E–02	2.01

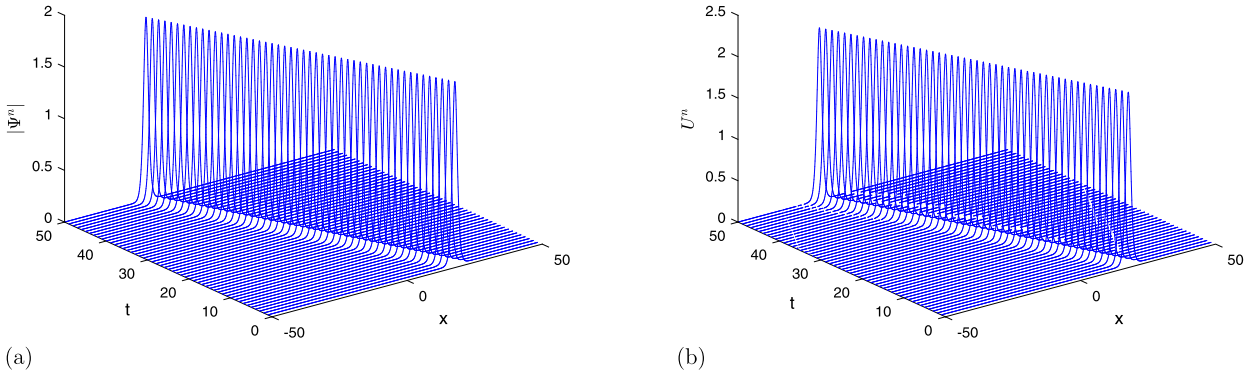

Fig. 5. Profiles of one soliton generated by four energy-preserving methods. (a): $|\Psi^n|$; (b): U^n.

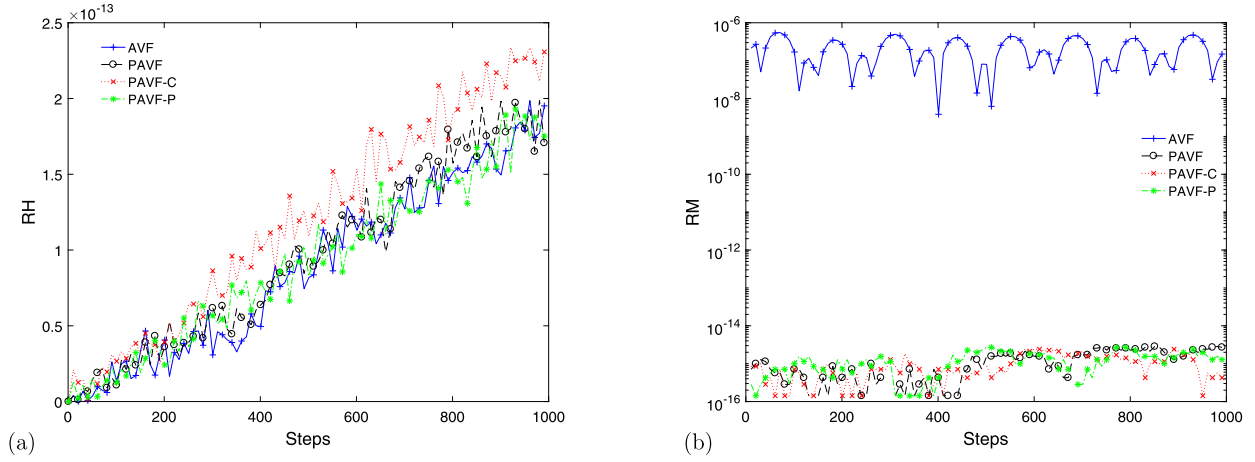

Fig. 6. Relative energy error RH (a) and mass error RM (b) of four energy-preserving methods for one soliton evolution.

Table 3
Computational cost of one solitons by four energy-preserving methods.

	AVF	PAVF	PAVF-C	PAVF-P
$h = 10/25$	3.47	1.86	3.02	3.26
$h = 10/50$	4.85	2.65	4.14	4.74
$h = 10/75$	7.19	3.45	5.39	6.89
$h = 10/100$	9.69	4.32	6.56	9.13
$h = 10/125$	11.93	4.33	6.58	9.40

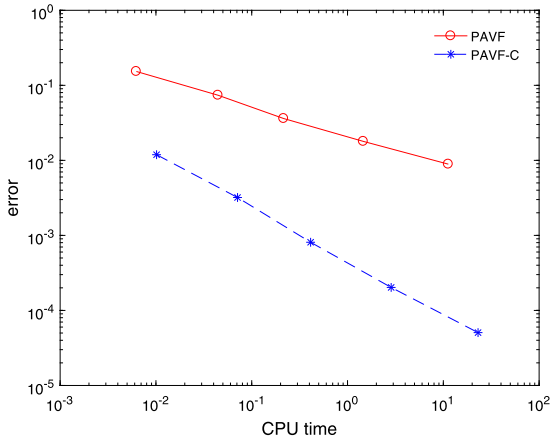

Fig. 7. Numerical errors versus computational costs of the PAVF method and the PAVF-C method at $t = 1$.

Next we consider the case of two colliding solitons with initial condition

$$\varphi(x,0) = \sum_{i=1}^{2}\left(\frac{3\sqrt{2}}{4\sqrt{1-c_i^2}}\operatorname{sech}^2\Big(\frac{1}{2\sqrt{1-c_i^2}}(x-x_i)\Big)\exp(ic_i x)\right),$$

$$u(x,0) = \sum_{i=1}^{2}\left(\frac{3}{4(1-c_i^2)}\operatorname{sech}^2\Big(\frac{1}{2\sqrt{1-c_i^2}}(x-x_i)\Big)\right),$$

$$u_t(x,0) = \sum_{i=1}^{2}\left(\frac{3c_i}{4(1-c_i^2)^{3/2}}\operatorname{sech}^2\Big(\frac{1}{2\sqrt{1-c_i^2}}(x-x_i)\Big)\tanh\Big(\frac{1}{2\sqrt{1-c_i^2}}(x-x_i)\Big)\right),$$

where $|c_i| < 1$, x_i, $i = 1, 2$ are the propagating velocities and initial phases of two solitons, respectively. We set $c_1 = -0.8, x_1 = 20$ and $c_2 = 0.8, x_2 = -20$ which corresponds to two colliding solitons with same amplitudes and speed but opposite directions and initial phases. The spatial and temporal steps are $h = 0.1, \tau = 0.05$. Fig. 8 demonstrates the evolution of shapes of $|\Psi^n|$ and U^n until $t = 50$ with clear collision observed. Although these profiles can be produced both by the original AVF method and our partitioned AVF methods, from the errors of discrete energy and mass in Fig. 9 our methods are superior in the exact conservation of these two invariants while the original method can only preserve the discrete energy. The computational costs of four methods with different spatial steps are listed in Table 4 which reveal a similar result as that in Table 3.

Notice that when the computing scale increases, the advantage of the PAVF method (3.14) becomes more evident. Therefore, we further present a numerical example about the following two-dimensional Klein–Gordon–Schrödinger (KGS) equation:

$$\begin{aligned} &i\varphi_t + \frac{1}{2}\Delta\varphi + u\varphi = 0,\\ &u_{tt} - \Delta u + u - |\varphi|^2 = 0, \end{aligned} \qquad \boldsymbol{x} \in [-10,10]\times[-10,10],\ t > 0, \tag{3.21}$$

with the same homogeneous Dirichlet boundary condition. The second-order central difference method is used to discretize the Laplace operators in both directions. The corresponding AVF, PAVF, PAVF-C and PAVF-P schemes are just similar to (3.12), (3.14), (3.19) and (3.20), respectively.

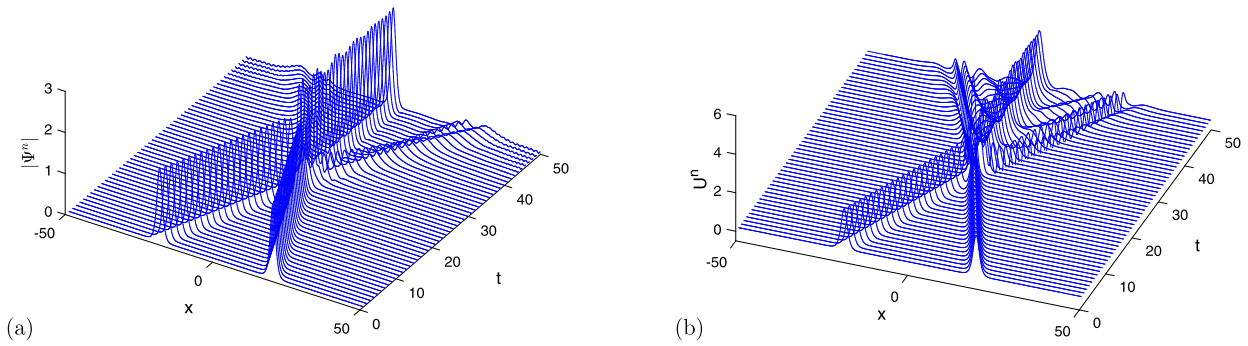

Fig. 8. Collisions of two solitons generated by four energy-preserving methods. (a): $|\Psi^n|$. (b): U^n.

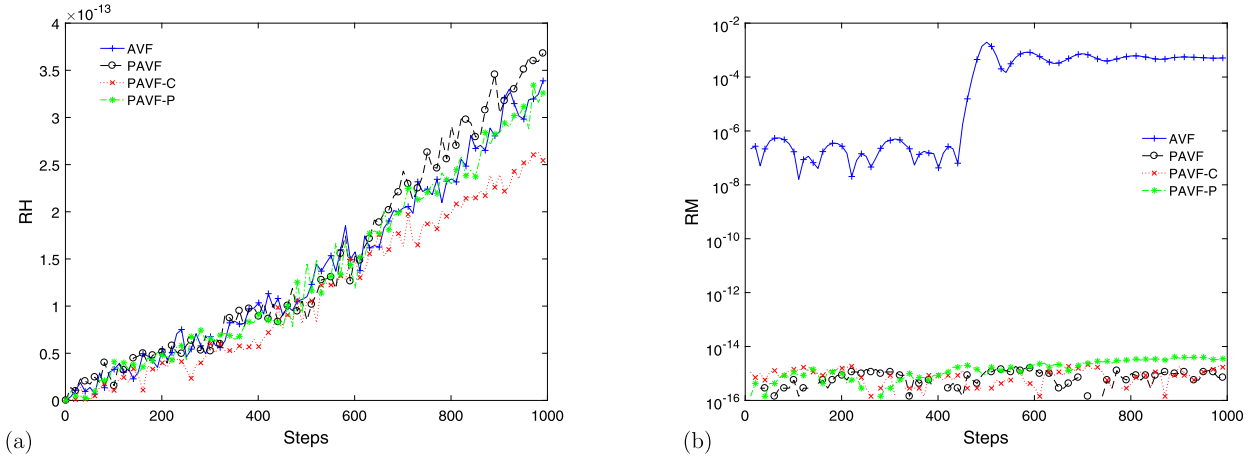

Fig. 9. Relative energy error RH (a) and mass error RM (b) of the four energy-preserving methods for two solitons evolution.

Table 4
Computational cost of two solitons by four energy-preserving methods.

	AVF	PAVF	PAVF-C	PAVF-P
$h = 10/25$	3.36	1.90	2.89	3.22
$h = 10/50$	4.79	2.52	4.04	4.80
$h = 10/75$	7.07	3.36	5.19	6.69
$h = 10/100$	9.62	4.24	6.65	9.24
$h = 10/125$	11.74	5.30	7.84	11.31

We take the initial conditions as

$$\phi(\boldsymbol{x}, 0) = (1 + i)\exp(-|\boldsymbol{x}|^2), \quad u(\boldsymbol{x}, 0) = \operatorname{sech}(|\boldsymbol{x}|^2), \quad u_t = \sin(x + y)\exp(-2|\boldsymbol{x}|^2).$$

We run this numerical test for every method and found that the obtained results are almost the same. Therefore, we just present the results of PAVF in Fig. 10 at $t = 0, 1, 2$, which uniformly show a correct time evolutions compared to the results in [23]. To demonstrate the computational efficiency of the PAVF method, we choose different mesh sizes and list the time cost for all the methods in Table 5. As expected, the PAVF method requires the smallest computational cost, regardless of its first-order accuracy. Among the second-order ones, the PAVF-C method is much more efficient than the PAVF-P method and the most time-consuming AVF method. As a consequence, the PAVF-C method is obviously the optimal choice among the four energy-preserving methods which will exhibit greater advantages of lower computational cost in simulating three-dimensional problems.

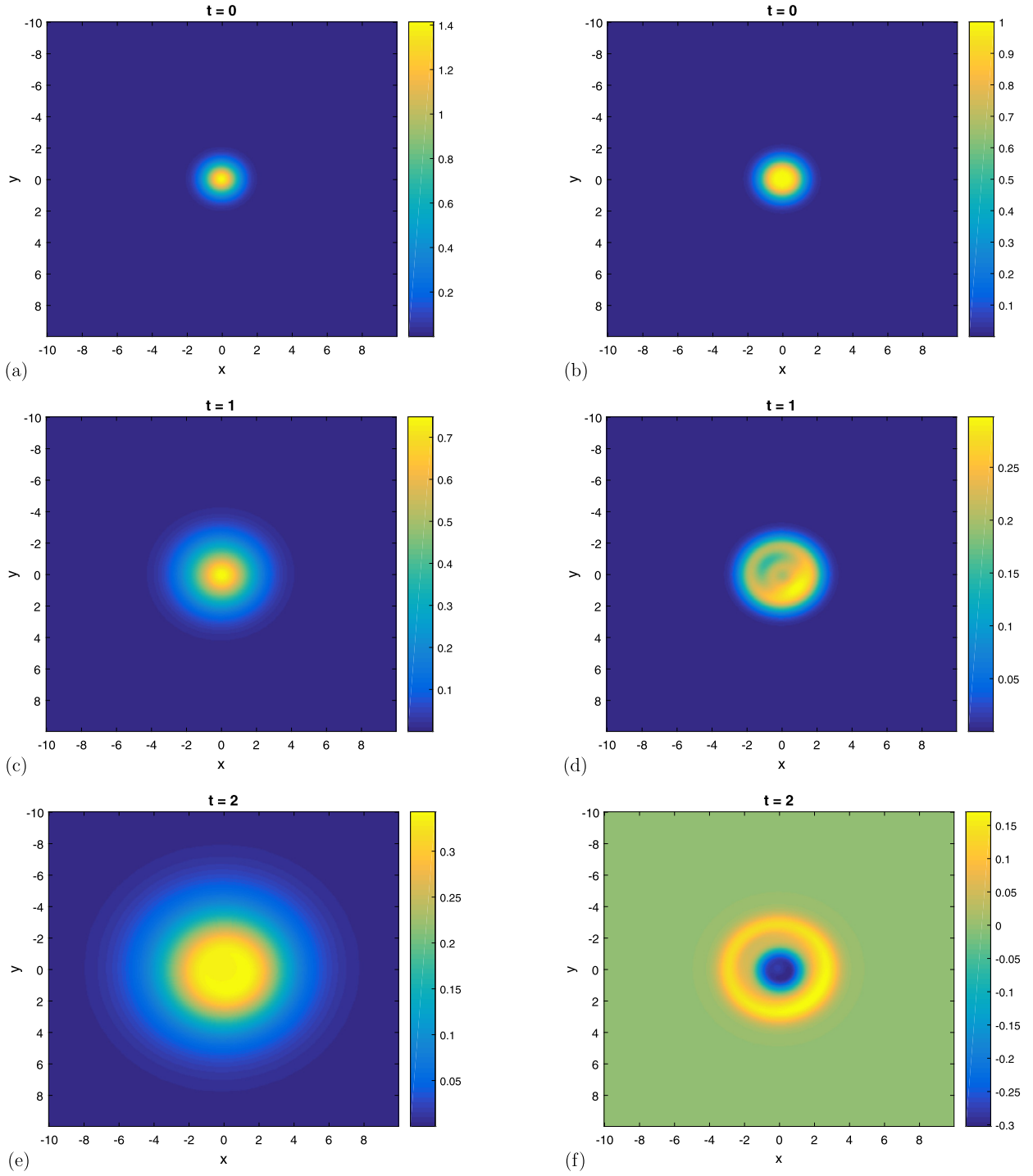

Fig. 10. Snapshot of $|\Psi^n|$ (left) and U^n (right) by four energy-preserving methods at $t = 0, 1, 2$.

4. Conclusions

We have presented a partitioned AVF method for Hamiltonian ODEs and PDEs which differs from the conventional AVF method in the derivation of the vector of means of the tangential components in the gradient of the Hamiltonian. Taking the Hénon–Heiles system and the Klein–Gordon–Schrödinger equation for examples, we demonstrate the advantages of the PAVF methods. With the grouping strategy, the resulting schemes are semi-implicit or linearly implicit. Consequently, such

Table 5
Computational cost of the two-dimensional example by four energy-preserving methods.

	AVF	PAVF	PAVF-C	PAVF-P
$h = 2/10$	5.70	1.70	5.54	5.91
$h = 2/20$	44.32	25.36	39.14	43.63
$h = 2/30$	107.70	29.46	87.82	103.03
$h = 2/40$	245.26	62.26	198.33	229.78
$h = 2/50$	744.35	385.77	631.57	719.94

schemes can decrease the computational scale or even avoid the nonlinear iteration process which has to be implemented by the original AVF method.

In addition, we further find that the partitioned AVF method can preserve extra conservative quantities besides the Hamiltonian energy in particular problem while the AVF method cannot, which deserves further investigation on other systems. When considering all variables as one group, the PAVF method just becomes the standard AVF method. In another extreme when each variable is viewed as an individual group, then the PAVF method is actually equivalent to the discrete gradient method.

For sake of improving the accuracy of the original partitioned AVF method, in conjunction with its adjoint, we further introduce the partitioned AVF composition method and plus method. Both the two modifications inherit the energy conservative property. However, the partitioned AVF composition method is more efficient than the plus method. Therefore, in practice the partitioned AVF composition method is a convenient alternative to the conventional AVF method.

Acknowledgements

This work is supported by the National Key Research and Development Project of China (2016YFC0600310), the National Natural Science Foundation of China (Grant Nos. 11771213, 41504078), the Jiangsu Collaborative Innovation Center for Climate Change and the Priority Academic Program Development of Jiangsu Higher Education Institutions.

References

[1] Z. Ge, Equivariant symplectic difference schemes and generating functions, Phys. D 49 (1991) 376–386.
[2] P. Chartier, E. Faou, A. Murua, An algebraic approach to invariant preserving integrators: the case of quadratic and Hamiltonian invariants, Numer. Math. 103 (2006) 575–590.
[3] L. Brugnano, F. Iavernaro, D. Trigiante, Energy- and quadratic invariants-preserving integrators based upon Gauss collocation formulae, SIAM J. Numer. Anal. 50 (2012) 2897–2916.
[4] J.M. Sanz-Serna, M.P. Calvo, Numerical Hamiltonian Problems, Chapman & Hall, London, 1994.
[5] B. Leimkuhler, S. Reich, Simulating Hamiltonian Dynamics, Cambridge University Press, Cambridge, 2004.
[6] E. Hairer, C. Lubich, G. Wanner, Geometric Numerical Integration: Structure-Preserving Algorithms for Ordinary Differential Equations, 2nd edition, Springer-Verlag, Berlin, 2006.
[7] S. Blanes, F. Casas, A Concise Introduction to Geometric Numerical Integration, CRC Press, Boca Raton, FL, 2016.
[8] L. Brugnano, F. Iavernaro, Line Integral Methods for Conservative Problems, CRC Press, Boca Raton, FL, 2016.
[9] E. Hairer, Symmetric projection methods for differential equations on manifolds, BIT 40 (2000) 726–734.
[10] R.I. McLachlan, G.R.W. Quispel, N. Robidoux, Geometric integration using discrete gradient, Phil. Trans. R. Soc. 357 (1999) 1021–1045.
[11] G.R.W. Quispel, D.I. McLaren, A new class of energy-preserving numerical integration methods, J. Phys. A, Math. Theor. 41 (2008) 045206.
[12] L. Brugnano, F. Iavernaro, D. Trigiante, Hamiltonian boundary value methods (energy preserving discrete line integral methods), J. Numer. Anal. Ind. Appl. Math. 5 (2010) 17–37.
[13] T. Matsuo, Dissipative/conservative Galerkin method using discrete partial derivatives for nonlinear evolution equations, J. Comput. Appl. Math. 218 (2008) 506–521.
[14] E. Celledoni, R.I. McLachlan, D. McLaren, B. Owren, G.R.W. Quispel, W.M. Wright, Energy preserving Runge–Kutta methods, M2AN 43 (2009) 645–649.
[15] E. Hairer, Energy preserving variant of collocation methods, J. Numer. Anal. Ind. Appl. Math. 5 (2010) 73–84.
[16] E. Celledoni, R.I. McLachlan, B. Owren, G.R.W. Quispel, Energy-preserving integrators and the structure of B-series, Found. Comput. Math. 10 (2010) 673–693.
[17] E. Celledoni, B. Owren, Y.J. Sun, The minimal stage, energy preserving Runge–Kutta method for polynomial Hamiltonian systems is the averaged vector field method, Math. Comput. 83 (2014) 1689–1700.
[18] E. Celledoni, V. Grimm, R.I. Mclachlan, D.I. McLaren, D. O'Neale, B. Owren, G.R.W. Quispel, Preserving energy resp. dissipation in numerical PDEs using the "Average Vector Field" method, J. Comput. Phys. 231 (2012) 6770–6789.
[19] T. Itoh, K. Abe, Hamiltonian-conserving discrete canonical equations based on variational difference quotients, J. Comput. Phys. 77 (1988) 85–102.
[20] E.E. Zotos, Classifying orbits in the classical Hénon–Heiles Hamiltonian system, Nonlinear Dyn. 79 (2015) 1665–1677.
[21] J.L. Hong, S.S. Jiang, C. Li, Explicit multi-symplectic methods for Klein–Gordon–Schrödinger equations, J. Comput. Phys. 228 (2009) 3517–3532.
[22] J.J. Zhang, L.H. Kong, New energy-preserving schemes for Klein–Gordon–Schrödinger equations, Appl. Math. Model. 40 (2016) 6969–6982.
[23] T.C. Wang, X.F. Zhao, J.P. Jiang, Unconditional and optimal H^2-error estimates of two linear and conservative finite difference schemes for the Klein–Gordon–Schrödinger equation in high dimensions, Adv. Comput. Math. 5 (2017) 1–27.